The confluence of aberration correction, spectroscopy and multi-dimensional data acquisition

Nestor J. Zaluzec

Argonne National Laboratory, Materials Science Div, Electron Microscopy Center, Argonne, IL, 60439 USA

Zaluzec@aaem.amc.anl.gov
Keywords: AEM, XEDS, EELS, Tomography, Aberration Correction, In-Situ, 3D/4D, Spectroscopy

In the last decade aberration correction has dramatically improved the imaging capabilities of our modern Transmission/Scanning Transmission Electron Microscopes. While the results have been enormously impressive, for the most part the impact of this technology on spectroscopy or thick specimens has been neglected. Traditionally the role of aberration correctors have concentrated upon improvements in "atomic" resolution, either derived by Cs correction of electron scattering or the ability to create smaller and more intense probes. Often neglected is the impact of the correctors on the geometrical configurations of lenses as well as the impact of improved collection on the various spectroscopic and imaging signals. Using uncorrected, Cs Only and Cs + Cc corrected operating modes of instruments operating under identical conditions we have begun a systematic evaluation of the benefits of correctors to both imaging in thick specimens as well as spectroscopic measurements.

In figure 1, we illustrate the results of imaging the same 5-30 nm diameter Au particles on a thick 500 nm SiN support in 3 different operating modes of 200 kV TEM instruments: uncorrected, Cs, and Cs+Cc corrected instruments [1]. This is done to assess the improvement aberration correction will afford thick specimen imaging as is typically encountered in high tilt angle tomographic TEM imaging or in closed cell in-situ stages. Not surprisingly, except for the case of STEM imaging of particles supported on the electron entrance surfaces (data not shown in this figure), the fully corrected Cs+Cc imaging systems provide the best imaging in thick specimens, Cs+Cc imaging is also markedly improved over simple EFTEM elastic imaging due to improved signal [1].

Traditionally, electron energy loss spectroscopy (EELS) is viewed as one of the most efficient means for microanalytical measurements in the analytical electron microscope. This perspective is based not only upon the physics of the signal generation process but also due to the relatively high geometrical signal collection efficiency of EELS relative to that used in conventional x-ray energy dispersive spectrometer (XEDS) geometries. Recent developments in silicon drift detectors (SDDs) have facilitated the construction of large solid angle x-ray spectrometers which when combined with the current generation of electron-optical instruments significantly impacts the performance of these analytical technologies. Figure 2 graphs the solid angle available to modern SDD as a function of detector area and distance from the specimen [2]. The new generation of commercial high solid angle detectors interfaced to today's instruments yields solid angles approaching 1 sR, and in experimental systems solid angles as high as 3 sR have achieved. Key to this new generation of detectors is their small size and the re-engineering of lens geometries to install either vary large and/or multiple detectors from directions which in the past were once not considered feasible. This facilitates x-ray geometrical detection efficiencies that are more than 10 times better than those considered good only a decade ago. Using these new configurations it becomes realistic to acquire large complex hyperspectral tomograms, which previously would have taken days in only a matter of a few hours. Figure 3, shows portions of a combined STEM image and XEDS elemental map of an In doped GaN LED structure [3]. Here we used hyperspectral imaging and the associated tomographic analysis to elucidate the elemental distribution of (In, Ga) N within these complex heterostructures. In this example, one can clearly visualize the outline of the truncated nanopyramid caps which have grown upon the seed GaN. Inspection of spectral imaging data we see the presence of the solid, coherent (In,Ga)N hexagonal pyramid with a heights of ~ 20 nm forming a GaInN quantum dot at the tip of each GaN nanopyramid.

The increased space afforded by correctors plus the improved efficiency in collection results in measurable improvement in signal and sensitivity in TEM, EFTEM and XEDS. The use of post-

specimen aberration correctors to simple EELS spectroscopy has shown little to no improvement in edge/background .

References

[1] N.J. Zaluzec *et al* . Proceedings of Microsc. Microanal 2012, Phoenix Az. in press
[2] N.J. Zaluzec Microsc. Microanal. **15**, 93–98, 2009
[3] Wildeson I.H. *et al* J. Appl. Phys. **108**, 044303 (2010); doi:10.1063/1.346699

[4] Research supported at ANL by US DOE Office of Science, Contract DE-AC02-06CH11357

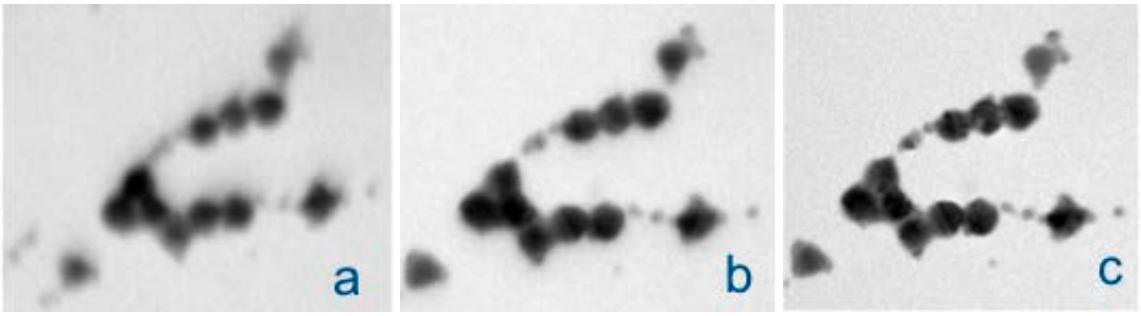

Figure 1. *TEM imaging of Au nanoparticles on 500nm SiN amorphous film for three different conditions a.) Cs =1.2 mm Cc =1.2 mm b.) Cs =2.03µm Cc = 1.83mm c.) Cs =2.01µm Cc = 0.46µm [1]*

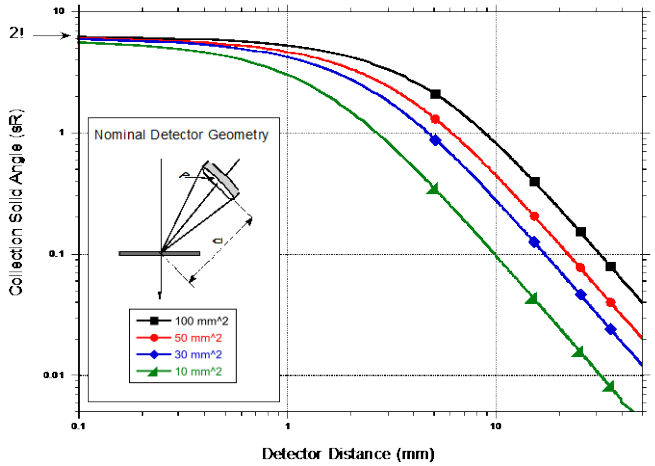

Figure 2. *Collection Solid Angle for a Solid State Energy Dispersive Spectrometer as a function of distance for various detector sizes. The maximum collection efficiency of a hemispherical detector is 2π sR.*

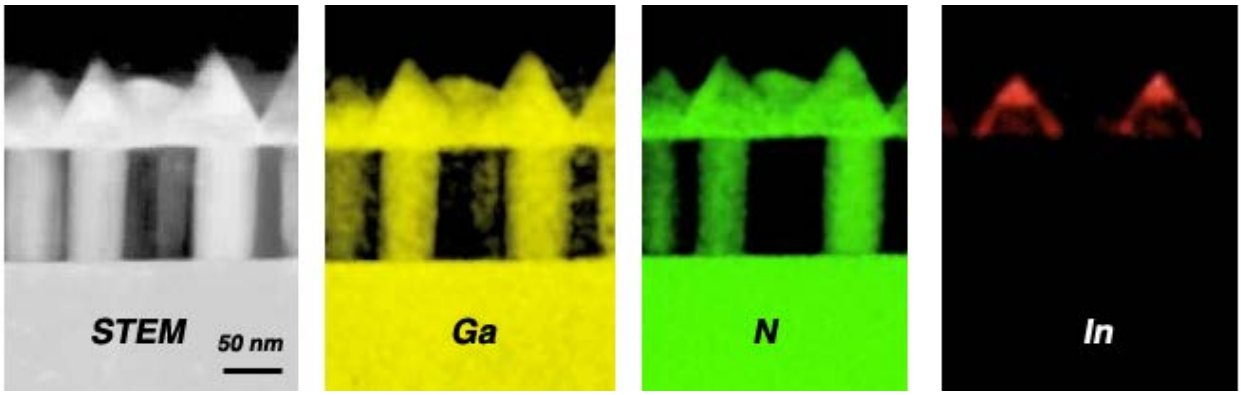

Figure 3. *Extracted images from a 3D XEDS hyperspectral imaging/tomographic measurement of the elemental distribution in In -doped GaN LED structures. Acquisition time for tomogram ~ 8 hours ($\pm 60^{o}$ in 3^{o} steps on 2 orthogonal axes, Data = 80 (1Kx1K) XEDS maps & 80 STEM images, 1 nA beam current)*

Aberration correction in digital holographic microscopy (DHM), however, has only been demonstrated for nonbiological samples or â€œthinâ€ biological samples (e.g., a single cell) using discrete-wavelength optical sources, and not for broadband tomography of bulk biological tissue.Â In this paper, we present a method for post-data-acquisition aberration correction that computationally modifies the effective pupil phase profile corresponding to the complex PSF of an OCT system, and demonstrate tomographic imaging of bulk biological tissue with computational aberration correction. Zaluzec NJ (2012) The Confluence of Aberration Correction, Spectroscopy and Multi-Dimensional Data Acquisition. Proc. European Microscopy CongressGoogle Scholar. 17.4 â€“ Atomic Resolution X-ray Analysis. Watanabe M (2013) Microscopy Hacks: Development of Various Techniques to Assist Quantitative Nanoanalysis and Advanced Electron Microscopy. Microscopy 62(2):217â€“241CrossRefGoogle Scholar. 17. Appendix 2 â€“ Calculation of Specimen Density. Three-Dimensional and Multidimensional Microscopy: Image Acquisition and Processing XVIII, edited by Jose-Angel Conchello, Carol J. Cogswell, Tony Wilson, Thomas G. Brown, Proc. of SPIE Vol. 7904. 790413 Â· Â© 2011 SPIE Â· CCC code: 1605-7422/11/$18 Â· doi: 10.1117/12.875907.Â The use of computers in radioisotope imaging is now well established for data acquisition, data correction, image reconstruction, image display and manipulation, data storage, system control and multimodal imaging and registration. This paper reviews these areas highlighting some of the applications and demands on computing facilities.